p210 bcr-abl induces amoeboid motility by recruiting ADF/destrin through RhoA/ROCK1

Tristan Rochelle, Thomas Daubon, Marleen van Troys, Thomas Harnois, Davy Waterschoot, Christophe Ampe, Lydia Roy, Nicolas Bourmeyster, Bruno Constantin

p210$^{bcr\text{-}abl}$ induces amoeboid motility by recruiting ADF/destrin through RhoA/ROCK1

Tristan Rochelle,*,[1] Thomas Daubon,*,[1,2] Marleen Van Troys,‡,§ Thomas Harnois,†,‖ Davy Waterschoot,‡,§ Christophe Ampe,‡,§ Lydia Roy,*,‖,¶ Nicolas Bourmeyster,*,†,‖,[3,4] and Bruno Constantin*,[3]

*Institut de Physiologie et Biologie Cellulaires, Unité Mixte de Recherche (UMR) Centre National de la Recherche Scientifique (CNRS) 6187, and †Plateforme de Protéomique ProteomeUP, Université de Poitiers, Poitiers, France; ‡Department of Biochemistry, Faculty of Medicine and Health Sciences, Ghent University, Gent, Belgium; §Department of Medical Protein Research, Vlaams Instituut voor Biotechnologie (VIB), Gent, Belgium; ‖Centre Hospitalier Universitaire de Poitiers, Poitiers, France; and ¶Institut National de la Santé et de la Recherche Médicale (INSERM) CIC-802, Poitiers, France

ABSTRACT **We previously demonstrated that the Bcr-Abl oncogene, p210$^{bcr\text{-}abl}$, through its unique GEF domain, specifically activates RhoA and induces spontaneous amoeboid motility. We intend to study the pathways downstream RhoA controlling amoeboid motility. Mouse prolymphoblastic cells (Ba/F3 cell line) expressing different forms of Bcr-Abl were embedded in 3-dimensional (3D) Matrigel to study motility and explore the effects of inhibiting Rho pathway (inhibitors and siRNAs). The phosphorylation levels of cofilin-1 and destrin were analyzed by 2-dimensional electrophoresis. Composition of Bcr-Abl signalplex in different conditions was determined by coimmunoprecipitation. Ba/F3p190 and Ba/F3 expressing a mutant form of p210$^{bcr\text{-}abl}$ (unable to activate RhoA) cells presented a spontaneous motility, but not an amoeboid type. p210$^{bcr\text{-}abl}$-induced amoeboid motility in a 3D matrix requires isoform-specific RhoA/ROCK-1/destrin signaling. Next to the conventional Rho/ROCK/MLC/myosin pathway, this pathway is a crucial determinant for amoeboid motility, specific for the destrin isoform (and not its coexpressed homologue cofilin-1). Also, the presence of destrin (and not cofilin-1) in the p210$^{bcr\text{-}abl}$ complex is dependent on ROCK1, and this signalplex is required for amoeboid motility. This underscores isoform-specific function within the ADF/cofilin family and provides new insight into Bcr-Abl signaling to amoeboid motility and possible impact on understanding chronic myeloid leukemia progression.—Rochelle, T., Daubon, T., Van Troys, M., Harnois, T., Waterschoot, D., Ampe, C., Roy, L., Bourmeyster, N., Constantin, B. p210$^{bcr\text{-}abl}$ induces amoeboid motility by recruiting ADF/destrin through RhoA/ROCK1. *FASEB J.* 27, 123–134 (2013). www.fasebj.org**

Key Words: isoform selectivity · cell migration · GTPases · actin-binding proteins · signalplex · leukemia

THE BCR-ABL ONCOGENE IS generated by a reciprocal translocation between chromosomes 9 and 22 (Philadelphia chromosome, Ph$^+$) that leads to the fusion of the 5′ region of the *bcr* gene with the 3′ region of the *abl* gene. Among the Bcr-Abl variants (1), p210$^{bcr\text{-}abl}$ is usually responsible for chronic myeloid leukemia (CML; ref. 2) whereas p190$^{bcr\text{-}abl}$ is responsible for a subset of acute lymphoblastic leukemia (3). Both proteins exhibit enhanced and constitutive tyrosine kinase activity, which is the main mechanism of leukemogenesis (4, 5). Expression of Bcr-Abl has been shown to induce abnormal actin cytoskeleton remodeling leading to altered cytoskeleton function, such as increased motility, altered adhesion (6–8), and decreased response to SDF-1α, a chemokine constitutively secreted by bone marrow stromal cells (9–11). This may contribute to the premature release of lymphoid and myeloid progenitors (12) from bone marrow, which can spill into the blood and evolve outside the niche.

The Bcr-Abl forms p190$^{bcr\text{-}abl}$ and p210$^{bcr\text{-}abl}$ structurally differ in a Dbl homology (DH) or guanine exchange factor (GEF) domain and a pleckstrin homology (PH) domain that are only present in p210$^{bcr\text{-}abl}$ and not in p190$^{bcr\text{-}abl}$. The functional consequences of these supplemental domains on specific signaling paths in Bcr-Abl cells have not been fully explored.

Abbreviations: 2D, 2-dimensional; 3D, 3-dimensional; ADF, actin depolymerizing factor; CML, chronic myeloid leukemia; DH, Dbl homology; DIC, differential interference contrast; GEF, guanine exchange factor; MLC, myosin light chain; PH, pleckstrin homology; RT, room temperature; siRNA, small interfering RNA

[1] These authors contributed equally to this work.

[2] Current address: INSERM U1053 IECB, Université Bordeaux II, 33600 Pessac, France.

[3] These authors contributed equally to this work.

[4] Correspondence: UMR CNRS 6187, Université de Poitiers, Pôle Biologie-Santé, Bâtiment B36, 1, rue Georges Bonnet, 86022 Poitiers Cedex, France. Email: n.bourmeyster@chu-poitiers.fr

doi: 10.1096/fj.12-205112

This article includes supplemental data. Please visit *http://www.fasebj.org* to obtain this information.

In a previous study we showed that ectopic expression of Bcr-Abl in Ba/F3 cells triggers spontaneous motility, and in particular that p190$^{bcr\text{-}abl}$-expressing Ba/F3 cells adopt a rolling-type motility, whereas p210$^{bcr\text{-}abl}$-expressing cells display amoeboid motility (13). Moreover, we demonstrated that RhoA is specifically activated by the GEF domain of p210$^{bcr\text{-}abl}$ (13, 14), promoting amoeboid movements. This is supported by the absence of amoeboid motility in Ba/F3 cells expressing p210S509A$^{bcr\text{-}abl}$, containing a mutation in the Rho-GEF domain, which, similar to p190$^{bcr\text{-}abl}$, does not activate RhoA.

A central role for Rho GTPases has been described in the molecular processes driving actin remodeling (15–18). Initially, most studied models of cell motility have relied on 2-dimensional (2D) mesenchymal motility that can be summarized by the following sequence of events: filopodial and lamellipodial membrane projections allow polarization, extension, and adhesion of the leading edge, then contraction of stress fibers in the cell body and rear detachment lead to a global forward movement (17, 18). Recently, based on 3-dimensional (3D) observations, amoeboid motility came back into focus as a main migration mode for a large variety of cells (19). Classically, amoeboid motility consists of deformation of the cell body generated by coordinated focal depolymerization and global contraction of the cortical actin (20), but the underlying molecular mechanisms are still far from clear. Although many epithelial or mesenchymal tumor cells have recently been shown to undergo amoeboid transition under specific conditions, amoeboid motility is assumed to be mainly used by hematopoietic cells (21, 22). However, few hematopoietic models have been described, and our previous data (13, 14) prove p190$^{bcr\text{-}abl}$- or p210$^{bcr\text{-}abl}$-expressing Ba/F3 cells to be suitable models. Amoeboid motility in a 3D matrix is currently mainly attributed to the activation of the RhoA/ROCK/myosin light chain (MLC)/myosin II pathway (23–25); however, the role of other effectors downstream of RhoA/ROCK, such as the actin depolymerizing factor (ADF)/cofilin family of actin modulators, is less understood.

In the present work, we unravel a second main amoeboid motility signaling pathways in Bcr-Abl-expressing cells: downstream of RhoA, ROCK1 and not ROCK2 specifically define this motility type. We show that the commitment to amoeboid motility renders the cell motility more efficient and show it crucially requires the specific recruitment of the ADF/cofilin family member ADF/destrin (and not cofilin-1) to the Bcr-Abl complex.

MATERIALS AND METHODS

Cells

The Ba/F3 cell line (ACC 300) was purchased from DSMZ (Braunschweig, Germany) and maintained in RPMI containing 10% FBS (Gibco BRL; Fisher Scientific, Illkirch, France) and recombinant mouse IL-3 (Miltenyi Biotech, Paris, France) at a final concentration of 2.5 ng/ml.

Cell line generation and cell cloning

The stable Bcr-Abl-expressing cell lines Ba/F3p190, Ba/F3p210, and Ba/F3p210S509A were generated previously (13) and maintained in Ba/F3 medium without IL-3. For Ba/F3p210*myc*-CFL1 and Ba/F3p210*myc*-ADF cell line generation, Ba/F3p210 were transfected using an Amaxa Nucleofector device (Lonza AG, Basel, Switzerland)with the appropriate plasmid DNA. After a 48-h cell expansion, 15 μg/ml of blasticidinS (Invivogen; Cayla, Toulouse, France) was added in medium for 2 wk of selection. Cell lines used in this study were all clonally selected and chosen on the basis of protein expression.

Plasmids

For *myc*-ADF/destrin and *myc*-CFL1, mouse cDNA encoding ADF/destrin and cofilin-1 were cloned in pcDNA6 myc/His vector (Invitrogen; Life Technologies, St Aubin, France) using the *Hind*III/*Eco*RI sites.

Transfections

All transfections have been performed using the Amaxa Nucleofector Kit-V with the X-005 program (Lonza), following the manufacturer's protocol. Small interfering RNA (siRNA; 2–4 μg) or plasmid DNA (2 μg) was used for RNAi experiments and (stable) transfection, respectively. SiRNA transfection efficiencies (>90%) were controlled using the siRNA-associated dyes by FACS analysis with BD-FacsCanto-II (BD Biosciences, Pont-de-Claix, France). Decrease in protein expression level was followed for 48 h for ROCKs and 96 h for ADFs. All experiments were performed 48 h post-transfection at the point of maximal down-regulation.

Antibodies and reagents

Antibodies

The following antibiodies were used: anti-Abl (clone 8E9) was obtainted from Becton Dickinson (Pont-de-Claix, France); anti-Myc (clone 9E10), anti-ADF/destrin (GV-13), and anti-actin were from Sigma-Aldrich (Saint-Quentin Fallavier, France); anti-RhoA (clone 26C4), anti-ROCK1 (H-85), anti-ROCK2 (C-20), and anti-cofilin-1 (5) were from Santa-Cruz Biotechnology (Heidelberg, Germany); anti-MLC2 and anti-phospho-MLC2 (Ser19) were from Cell Signaling Technology (Ozyme, Montigny-Le-Bretonneux, France); and anti-MYPT1 and anti-phospho-MYPT1 (Thr696) were from Millipore (Molsheim, France). Secondary HRP-conjugated goat anti-mouse IgG and goat anti-rabbit IgG were obtained from GE Healthcare (VWR International, Strasbourg, France). Secondary HRP-conjugated rabbit anti-goat was purchased from Santa Cruz Biotechnology.

Reagents

The ROCK inhibitor Y27632 and the myosin II inhibitor blebbistatin were purchased from Sigma-Aldrich. Calf intestinal alkaline phosphatase was acquired from New England Biolabs (Evry, France). Labeled siRNAs corresponding to the target sequences of mouse mRNA of ROCK1, 5′(FI)-GCAAAGAGAUUGUUAGAAU-3′, ROCK2, 5′(DY547)-CAAUGAAGCUUCUUAGUAA-3′, ADF/Destrin, 5′(FI)-GUGAUUGCAAUCCGUGUAU-3′ from ref. 26, and cofilin-1, 5′(DY547)-CCAAGGAGAGCAAGAAGGA-3′, were ordered from Dharmacon (Abgene, Epsom, UK). Control 5′Cy5-labeled siRNA was purchased from Eurogentec (Angers, France).

Inhibitor studies

Cells were treated with ROCK inhibitor Y-27632 (10 μM) or with the myosin II inhibitor blebbistatin (25 μM) over 1 to 5 h.

Lysis, immunoprecipitations, SDS-PAGE, and immunoblots

Lysis, immunoprecipitation, SDS–PAGE, Western blotting, and immunodetection were performed as described previously (14). Absolute quantification of cofilin-1 and ADF in Ba/F3 cells was done using purified recombinant GST-mouse-cofilin-1 and GST-mouse-ADF as standards. Signals on Western blot on which a specific amount of protein (20–40 μg) of cell lysate and a concentration series of the purified protein (standards) migrated were compared.

Two-dimensional electrophoresis

Cells (1.5–2×10^6) grown in tissue culture plates were washed and directly lysed in 190 μl of Destreak buffer (7-6003-19; GE Healthcare) supplemented with 2 mM orthovanadate, 5% IPG buffer NL (pH 3–10; 17-6000-88, GE Healthcare), and a phosphatase inhibitor cocktail. The prepared lysates were passed several times through a syringe with a $25G^{5/8}$ needle before being clarified at 10,000 *g* for 10 min at room temperature (RT). Supernatants were then loaded onto 7 cm immobiline DryStrip 3-10NL (GE Healthcare) and allowed to rehydrate overnight. Isoelectric focusing was performed on a Multiphor II Electrophoresis system (GE Healthcare) for 156 min (1 min at 200 V, 90 min at 200-3500 V, and 65 min at 3500 V). The buffer was then exchanged twice on the strips by two 15-min soakings in *1*) 50 mM Tris (pH 8.8), 6 M urea, 30% glycerol, 2% SDS, 2 mg/ml DTT (Sigma-Aldrich), and 0.01% bromphenol blue buffer and *2*) 50 mM TrisHCl (pH 8.8), 6 M urea, 30% glycerol, 2% SDS, 5 mg/ml iodoacetamide (Sigma-Aldrich), and 0.01% bromphenol blue buffer. Strips were layered horizontally on 1-mm thickness 13% acrylamide SDS gels with a 0.4% agarose stacking gel for electrophoresis in the two dimensions. Immunoblotting was performed as described previously for 1-dimensional SDS-PAGE (14). For 2D immunoblots, the acid end of the pH gradient is positioned to the left, so the furthermost left spot corresponds to the phospho form as demonstrated by alkaline phosphatase treatment (Supplemental Fig. S2).

Time-lapse recordings in 3D Matrigel

Cells in RPMI 1640 supplemented with 10% FBS were mixed in liquid Matrigel (growth factor reduced; BD Biosciences) at 1 × 10^6 cells/ml in a 2 mg/ml final concentration of Matrigel. The mixture was cast into a 1-cm-diameter 2-mm-high Teflon ring on a 30-mm coverslip and incubated for 30 min at 37°C in a 5% CO_2 incubator. For inhibition studies, cells were pretreated for 1 h with 10 μM Y27632 or 25 μM blebbistatin before embedding into Matrigel. Cell imaging was done as described earlier (13). During the 30-min recording, cells were maintained in a controlled environment chamber (temperature, CO_2, H_2O), and 1 frame was taken every 5 s. Movies presented were shrunk to 1 min by a 60-fold acceleration (12 frames/s). For motility-type scoring, 200 to 600 cells for each cell type and condition were observed on the time-lapse recordings. The motility studies were first analyzed by T.R., who recorded the movies, then analyzed blindly and separately by B.C. and N.B. The final result presented in the figures is the average of the 3 analyses.

Immunofluorescence microscopy

Cells in Matrigel (3D)

Cells (1×10^5) were embedded in pure Matrigel in glass-bottom 3-cm dishes (MatTek Corp., Ashland, MA, USA) and allowed to polymerize for 30 min at 37°C. RPMI medium was then added, and the Matrigel-embedded cells were kept at 37°C for 24 h. The in-gel fixation was achieved by immersion (30 min, RT) in PBS containing 4% paraformaldehyde. Cells were permeabilized with 0.5% Triton X-100 for 1 h, and blocking was performed with 3% fetal bovine serum for 30 min (RT). The gels were incubated with primary antibodies (overnight, RT), then with the appropriate secondary Alexa Fluor-488 conjugated antibodies (3 h, RT). F-actin was stained at this step with phalloidin conjugated to Alexa Fluor-546. The gels were mounted by adding Fluoromount mounting medium and a coverslip on top.

To make 3D images, serial optical sections of cells were captured with the software's automatic scanning mode. *Z*-stack digital images were collected optically at every 0.2-μm depth, and saved and used for 3D reconstruction using the Imaris software (Bitplane, Zurich, Switzerland).

Cells in suspension

Ba/F3 cells were seeded in a 24-well plate at 5 × 10^5 cells/ml in RPMI. After sedimentation of the cells, 800 μl of medium was removed and replaced by PBS containing 4% paraformaldehyde. Fixation was performed for 20 min, then cells were collected and centrifuged, and the pellet was recovered in 150 μl of 1% PBS/BSA. A 35-μl drop was placed on a superfrost slide and dried under laminar flow. Cells were permeabilized with 0.3% Triton X-100 for 5 min, and blocking was performed with 3% fetal bovine serum for 15 min. Slides were incubated with primary antibodies (1 h), and then with the appropriate secondary Alexa Fluor-488 conjugated antibodies (3 h, RT). F-actin was stained at this step with phalloidin conjugated to Alexa Fluor-546. Slides were mounted by adding Mowiol mounting medium (Sigma) and a coverslip on top.

Cells were analyzed by confocal imaging using a Zeiss LSM 510 inverted laser scanning fluorescence microscope equipped with LSM 510 acquisition software (Carl Zeiss, Oberkochen, Germany) and a ×63, numerical aperture (NA) 1.4 oil-immersion objective. Double color imaging using Alexa 488-labeled secondary antibodies and Alexa 546-phalloidin was obtained using selective laser excitation at 488 and 543 nm, respectively. Each channel was imaged sequentially using the multitrack recording module before merging.

Statistical analysis

Results are expressed as means ± SE of *n* observations. Sets of data were compared with a Student's *t* test. Differences were considered statistically significant at values of $P < 0.05$. Densitometry was performed using Scion software (Scion Corp., Frederick, MD, USA).

RESULTS

p210$^{bcr\text{-}abl}$-induced amoeboid motility is driven through ROCK1 activation

We previously showed that p190$^{bcr\text{-}abl}$ and p210$^{bcr\text{-}abl}$ both induce spontaneous motility of Ba/F3 cells but

displayed differential motility modes. Ba/F3p190 cells present a crawling or rolling motility. The latter modes are characterized by an absence of cell body deformation and use short filopodia to displace the cell body. In the case of crawling motility, cell projections (sometimes lamellipodia-like) are at the leading edge and seem to pull at the cell body, with the latter remaining round during translocation (**Fig. 1*A***). It is important to note that during recording, a defined Ba/F3p190 cell can first use a rolling mode, then crawling, or *vice versa*. For this reason, we grouped both types in one category (see below), since cells migrate using both mobility processes. In contrast, Ba/F3p210 cells mainly display amoeboid motility characterized by the presence of one large pseudopodial protrusion at the leading edge that directs the movement, and a cell body that is continuously deforming mobilized through contraction (refs. 19, 27 and Fig. 1*A*). In absence of chemokines like SDF-1α, parental Ba/F3 cells are strictly nonmotile (28, 29). Tracking analysis of time-lapse recordings of Ba/F3 cells in 3D Matrigel demonstrates the absence of spontaneous motility of these cells (Fig. 1*B*). In contrast, both Ba/F3p190 and Ba/F3p210 cells display spontaneous motility, as previously shown (13). During the recording time (30 min), ~60% of Ba/F3p210 cells displayed spontaneous motility, compared to <30% for Ba/F3p190 cells (**Fig. 2*C***). For both migrating Ba/F3p190 and Ba/F3p210 cells, the mean net displacement is lower than the mean total track length, suggesting a nondirectional motility (Fig. 1*B*, *C*). Nevertheless, migrating Ba/F3p210 cells presented significantly longer tracks and net displacement than Ba/F3p190 in 3D Matrigel, suggesting a more efficient and persistent migration (Fig. 1*B*, *C*). The other major difference is that none of the motile Ba/F3p190 cells used amoeboid motility, whereas >70% of the Ba/F3p210 cells displayed this form of motility (Fig. 2*D*).

Amoeboid cell body deformation is typically associated with RhoA and ROCK activity. Our data are in accordance with previous results showing that RhoA is directly activated by the GEF domain of $p210^{bcr\text{-}abl}$, which is not present in $p190^{bcr\text{-}abl}$ (13). Interestingly, as monitored by MyPT1 phosphorylation, ROCK activity was detected only in Ba/F3p210 cells (Fig. 2*A*). We thus probed the presence of RhoA and ROCK family members in the Bcr-Abl complexes. RhoA and ROCK1 were observed only in complexes with $p210^{bcr\text{-}abl}$ and not with $p190^{bcr\text{-}abl}$ (Fig. 2*B* and Supplemental Fig. S1*A*). The presence of RhoA and ROCK1 requires a functional GEF domain in $p210^{bcr\text{-}abl}$ (Supplemental Fig. S1*A*). Intriguingly, ROCK2 was not detected in complex with $p210^{bcr\text{-}abl}$, although it is expressed in Ba/F3 cells (Fig. 2*B* and Supplemental Fig. S1*A*). As expected, neither ROCK1 nor ROCK2 was found in complexes with $p190^{bcr\text{-}abl}$ or $p145^{abl}$ (Fig. 2*B* and Supplemental Figs. S1*A* and S3*D*).

On treatment with the ROCK inhibitor Y27632, we observed in time-lapse recordings a clear diminution of the percentage of motile cells for Ba/F3p210 cells, while no modification of this parameter was observed for Ba/F3p190 cells (Fig. 2*C*). The changed motility in Ba/F3p210 cells was associated with a total loss of amoeboid movements and an almost complete conversion into the rolling- or crawling-type motility characteristic of Ba/F3p190 cells (Fig. 2*D* and Supplemental Movie S1). Using ROCK1 or ROCK2 isoform-specific siRNA (Supplemental Fig. S1*B*), we showed that the amoeboid motility of the $p210^{bcr\text{-}abl}$-expressing cells is specifically dependent on ROCK1, but not on ROCK2 (Fig. 2*E*). Based on time-lapse recordings and quantification of motility types, only 1.4% of Ba/F3p210 cells presented amoeboid motility after depletion of ROCK1 (*vs.* 68% in control cells), whereas knockdown of ROCK2 induced only a mild reduction of ~20% in amoeboid movement (Fig. 2*E*). Neither ROCK1-siRNA nor ROCK2-siRNA modified the motility mode of Ba/F3p190 cells (not shown). Taken together, these results demonstrate that the Bcr-Abl-induced amoeboid movements are specifically controlled by RhoA-ROCK1-activation.

We further explored the signaling pathways downstream of ROCK1. Most publications focusing on amoeboid motility describe the central role of myosin II activation through ROCK-induced MLC phosphorylation enhancement (30). Accordingly, we observed a high phosphorylation level of

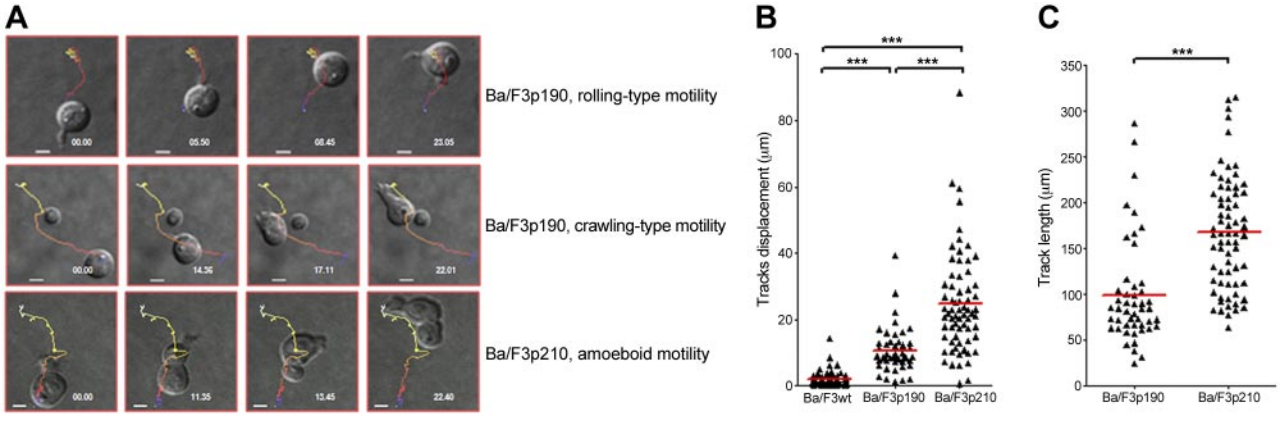

Figure 1. Morphological and physical characteristics of the different spontaneous motilities induced by $p190^{bcr\text{-}abl}$ and $p210^{bcr\text{-}abl}$. *A*) Morphological characterization of rolling-type (top panel), crawling-type (middle panel) or amoeboid-type (bottom panel) motilities using differential interference contrast (DIC) microscopy and track analysis. *B*, *C*) Cell-tracking analysis: Multiple tracks of individual Ba/F3wt, Ba/F3p190, and Ba/F3p210 cells were recorded by time-lapse video microscopy over 30 min using DIC microscopy. For each track, the net displacement between initial and final positions (*B*) and the total track length (*C*) were analyzed.

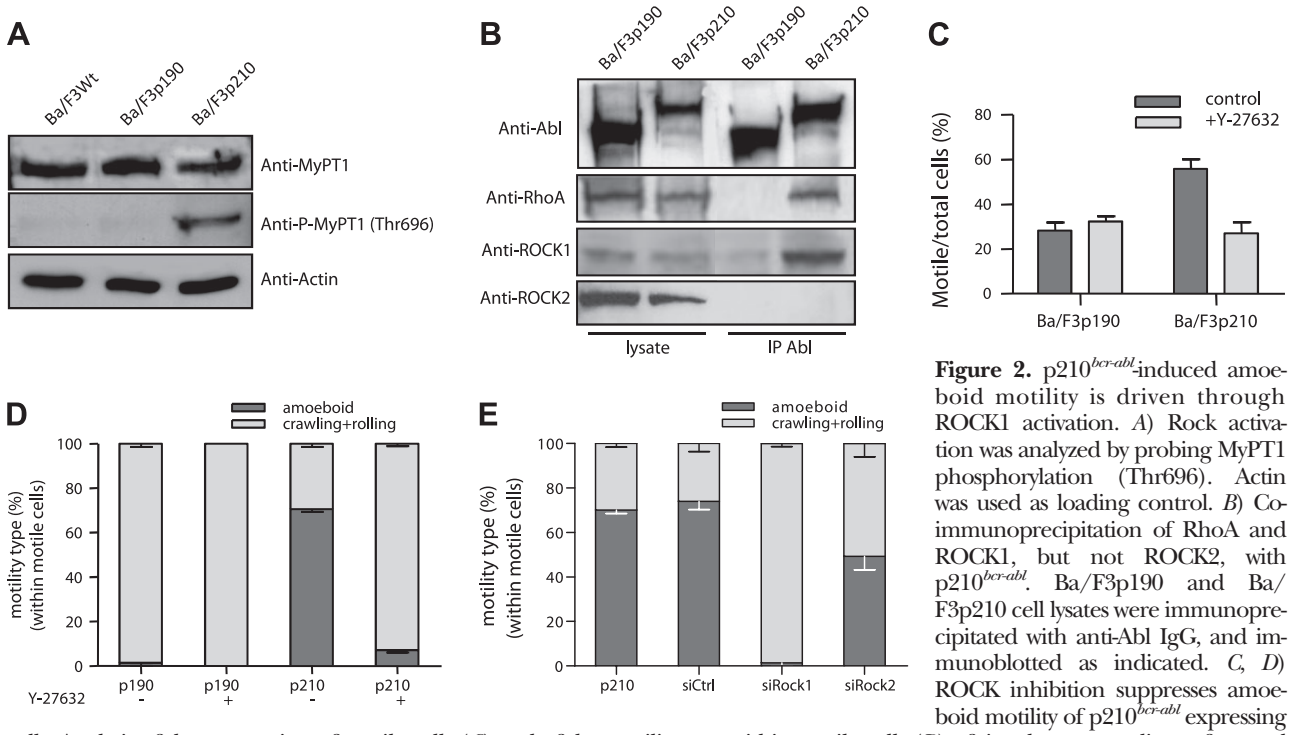

Figure 2. p210$^{bcr\text{-}abl}$-induced amoeboid motility is driven through ROCK1 activation. *A*) Rock activation was analyzed by probing MyPT1 phosphorylation (Thr696). Actin was used as loading control. *B*) Co-immunoprecipitation of RhoA and ROCK1, but not ROCK2, with p210$^{bcr\text{-}abl}$. Ba/F3p190 and Ba/F3p210 cell lysates were immunoprecipitated with anti-Abl IgG, and immunoblotted as indicated. *C, D*) ROCK inhibition suppresses amoeboid motility of p210$^{bcr\text{-}abl}$ expressing cells. Analysis of the proportion of motile cells (*C*) and of the motility type within motile cells (*D*) of time-lapse recordings of control and 10 μM ROCK Inhibitor Y27632 treated Ba/F3p190 and Ba/F3p210 cells in 3D Matrigel. *E*) ROCK1- or ROCK2-siRNA-transfected Ba/F3p210 cells. At 48 h after transfection with the indicated siRNA, Ba/F3p210 cells were embedded in 3D Matrigel, and time-lapse recording was performed using DIC microscopy. Phenotype of motile cells was analyzed and cells sorted in amoeboid or crawling/rolling motility type. Data are expressed as percentage of motile Ba/F3p190 and Ba/F3p210 cells with a specific motility type; 200-600 cells/condition were observed.

MLC in the Ba/F3p210 cells (dependent on a functional Rho GEF domain), compared to that in Ba/F3p190 cells (**Fig. 3*A***). Treatment with Y27632 induced total inhibition of this MLC phosphorylation (Fig. 3*B*). In accordance with results presented above (Fig. 2) demonstrating that only ROCK1 was involved in p210$^{bcr\text{-}abl}$ signal transduction, siRNA knockdown of ROCK1 induced a strong inhibition of MLC phosphorylation, whereas ROCK2 depletion had no effect (Fig. 3*C*). Blebbistatin treatment did not affect the rolling/crawling-type motility of the p190$^{bcr\text{-}abl}$ cells (not shown), but it drastically reduced amoeboid motility of the Ba/F3p210 cell population (Fig. 3*D* and Supplemental Movie S2). Myosin II activity thus strongly contributes to the amoeboid motility phenotype. However, other effectors downstream of RhoA-ROCK1 may also be involved. Since ADF/cofilins are the other main effectors regulated by Rho-ROCK (31), we decided to investigate this pathway.

ROCK1 controls cofilin-1 and ADF/destrin phosphorylation only in Ba/F3p210 cells

Cofilin-1 and ADF/destrin, two highly similar members of the ADF family, are coexpressed in most cells, and little is known on their specific roles in cell motility. Until now they have been usually considered as redundant (26, 31). Their actin-binding activity is regulated by phosphorylation and dephosphorylation of Ser3, with the dephosphorylated form being the active one. The upstream signaling of cofilin/ADF regulation is complex, with multiple kinases and phosphatases involved (31). Using specific antibodies, we first explored by Western blotting the expression levels of LIMK 1 and 2 , major cofilin and ADF kinases, and their phosphorylation levels in Ba/F3p190 and Ba/F3p210 cells. No statistical difference could be observed for any of these isoforms between p190$^{bcr\text{-}abl}$- and p210$^{bcr\text{-}abl}$-expressing cells (not shown). Cofilin-1 and ADF/destrin are both expressed at similar levels in Ba/F3p190 and Ba/F3p210 cells (**Fig. 4*A, B***). Since the cofilin-1/ADF ratio is reported to vary depending on cell type (32), we quantified the protein ratio of ADF to cofilin-1 in Bcr-Abl-expressing Ba/F3 cells, using purified bacterially produced cofilin-1 and ADF/destrin as standards (see Materials and Methods). This revealed that the ratio of cofilin-1 over ADF was ~1.5 ± 0.23 in both Ba/F3p190 and Ba/F3p210 cells.

In the absence of reliable and specific anti-phospho-ADF antibodies, we used 2D electrophoresis to explore cofilin-1 and ADF/destrin phosphorylation (see Supplemental Fig. S2 for identification of phosphorylated spots). Interestingly, whereas the cofilin-1 phosphorylated form is predominant in Ba/F3 parental cells a clear inhibition of cofilin-1 phosphorylation was observed in Ba/F3p190 and Ba/F3p210 cells (Fig. 4*C*). This was recently demonstrated to be a consequence of Bcr-Abl expression in Ba/F3 cells (29, 33). In contrast, the ADF/destrin phosphorylated form was present in Ba/F3wt, Ba/F3p190, and Ba/F3p210 cells (Fig. 4*C*). The ADF/destrin phosphorylation level is slightly decreased by 15% ($P<0.0027$) in Ba/F3p210 cells in comparison to Ba/F3p190 cells (Fig. 4*C*). The level of unphosphorylated ADF/cofilin family proteins was

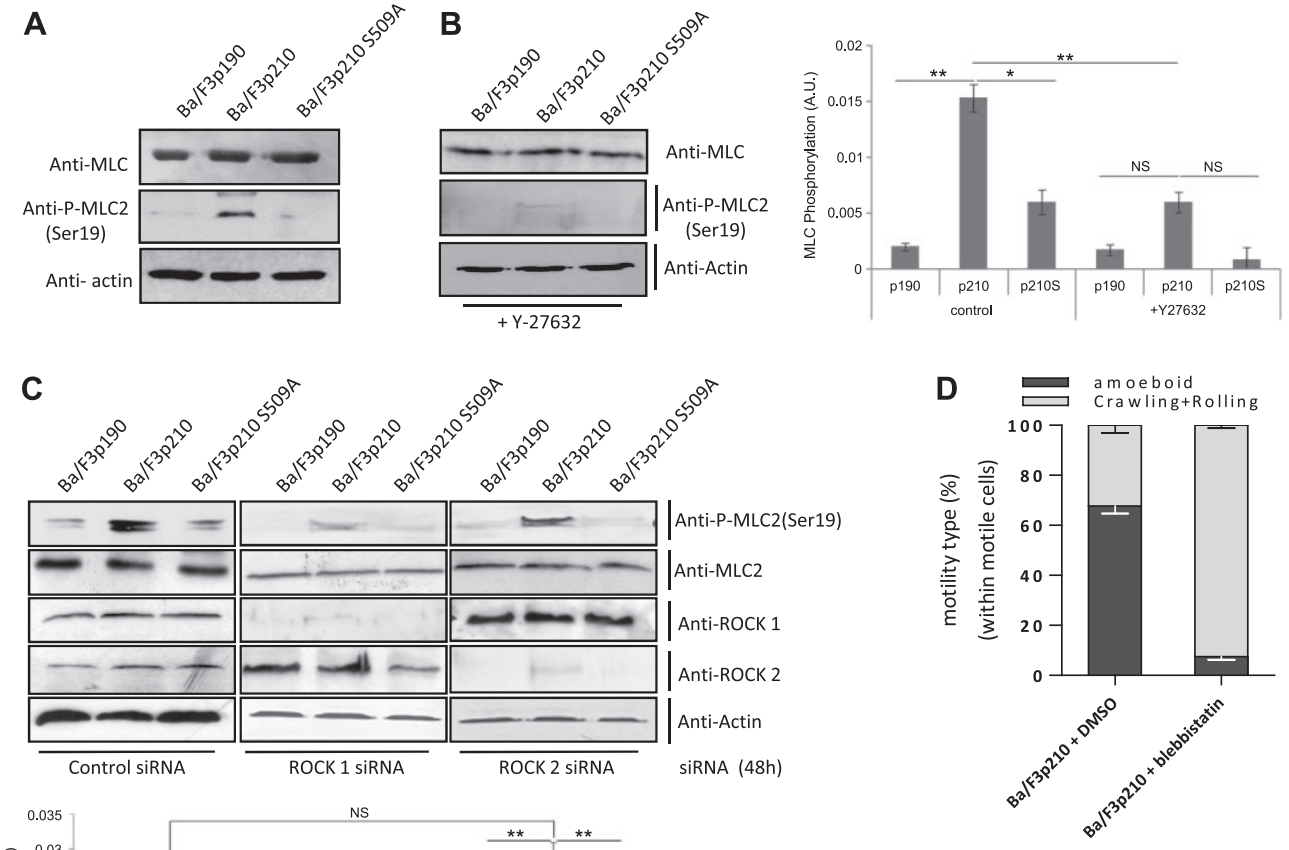

Figure 3. *A*) Phosphorylation state of MLC in Bcr-Abl-expressing cells. Ba/F3p190, BaF3p210, and Ba/F3p210S509A cells were lysed, and the levels of phospho-MLC and total MLC were detected by immunoblotting. Total actin was used as loading control. Results are representative of 1 experiment out of 3. *B*) Phosphorylation state of MLC in Bcr-Abl-expressing cells after 5 h of 10 μM Y-27632 treatment. Left panel: total proteins from Ba/F3p190, BaF3p210, and Ba/F3p210S509A were extracted and immunoblotted as indicated. Total actin was used as loading control. Right panel: P-MLC/MLC ratio. Histogram shows mean ± SE values of 3 independent experiments. *C*) Phosphorylation state of MLC in Bcr-Abl-expressing cells after ROCK1 or ROCK2 down-regulation; 48 h post-transfection with scramble or ROCK1 or ROCK2 siRNA, Ba/F3p190, BaF3p210 and Ba/F3p210S509A were lysed and phosphorylation state of MLC was determined by immunoblotting. Total actin was used as loading control. *D*) Myosin inhibition decreases amoeboid motility. Analysis of time-lapse recordings of control or blebbistatin-treated Ba/F3p210 cells. At 1 h after treatment with 25 μM blebbistatin, Ba/F3p210 cells were embedded into 3D Matrigel, and time-lapse recordings were performed using DIC microscopy. Motile cell phenotype was analyzed, and cells were sorted in amoeboid or crawling/rolling motility type. Data are expressed as percentage of motile Ba/F3p210 cells (200–300 cells/condition were observed).

demonstrated to be responsible for efficient migration and invasion of a mammary carcinoma cell line (34). Although statistically significant, this slight difference in ADF phosphorylation state is unlikely to explain the presence of an amoeboid motility mode only in Ba/F3p210 cells.

Using the ROCK inhibitor Y27632, we explored the ROCK dependency of the phosphorylation of cofilin-1 and ADF/destrin. In line with the fact that no ROCK activity was present in Ba/F3p190 cells, modification of the phosphorylation level of cofilin-1 and ADF/destrin was not observed in these cells on ROCK inhibition. In contrast, in Ba/F3p210 cells, Y27632 treatment induced an increase in cofilin-1 phosphorylation and a decrease in ADF/destrin phosphorylation (**Fig. 5*A, B***). Similar results were obtained using ROCK1-siRNA in Ba/F3p210 cells, whereas ROCK2-siRNA induced no modification in the level of phosphorylation of cofilin-1 or ADF/destrin in this cell line (Fig. 5*C, D*). These results highlight an isoform specificity of ROCK1 toward ADF/cofilin family proteins. Moreover, they indicate that ROCK1 activity is responsible for ADF/destrin phosphorylation in Ba/F3p210 cells that display amoeboid motility.

ADF/destrin is present in complex with p210$^{bcr\text{-}abl}$ only

The results presented above do not strongly support a determinant role of phosphorylation of ADF/destrin or cofilin-1 in the commitment to the different modes of motility. We thus explored the differential interactions of these protein isoforms in the context of macromolecular complexes organized around Bcr-Abl. We

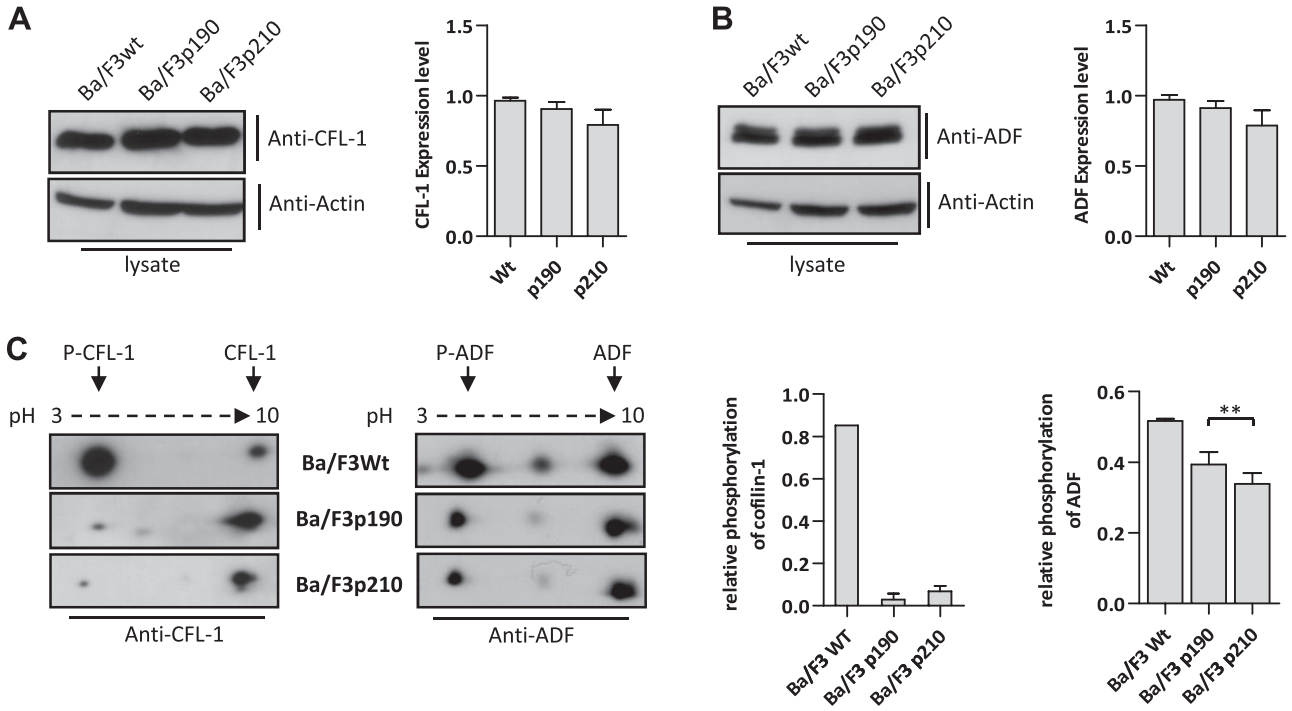

Figure 4. Protein levels of ADF/cofilins are not modified downstream of Bcr-Abl, but phosphorylation levels vary. *A*, *B*) Cofilin-1 (*A*) and ADF/destrin (*B*) protein level in Bcr-Abl-expressing and WT Ba/F3 cells. Total proteins from Ba/F3wt, Ba/F3p190, and Ba/F3p210 were extracted and immunoblotted as indicated. Actin was used as loading control. *C*) 2D-PAGE followed by Western blot analysis of Ba/F3wt, Ba/F3p190, and Ba/F3p210 cell extracts. Phosphorylated and unphosphorylated forms of cofilin-1 and ADF/destrin were detected by immunoblotting. Right panels show densitometric analysis of immunoblots (n=4).

showed above (Fig. 2*B* and Supplemental Figs. S1*A* and S3*D*) that the complex around p210$^{bcr\text{-}abl}$specifically contained activated RhoA and ROCK1. We explored the presence of either cofilin-1 or ADF/destrin in complex with p210$^{bcr\text{-}abl}$ using coimmunoprecipitation assays with anti-Abl, anti-cofilin-1, or anti-ADF/destrin antibodies. Cofilin-1 was not present in complex with any form of Bcr-Abl. In contrast, we found that ADF/destrin is present in complex with p210$^{bcr\text{-}abl}$ and absent in complex with p190$^{bcr\text{-}abl}$ (**Fig. 6*A***). We performed 2D gel electrophoresis experiments to determine whether phosphorylated and/or unphosphorylated ADF/destrin was present in complex with p210$^{bcr\text{-}abl}$. Interestingly, 2D electrophoresis of anti-Abl immunoprecipitation from Ba/F3p210 cells revealed that both forms of ADF/destrin were present in complex with p210$^{bcr\text{-}abl}$ (Fig. 6*B*). The phospho-ADF/ADF ratio in the whole-cell lysate and in the immunoprecipitated complex was highly similar.

Interestingly, the presence of ADF/destrin in complex with p210$^{bcr\text{-}abl}$ was dependent on the presence of ROCK but not on its activity, as demonstrated by coimmunoprecipitation assays after treatment with the ROCK inhibitor Y27632 (Fig. 6*C*) or ROCK1 siRNA (Fig. 6*D*). As a control, ROCK2 knockdown did not change the presence of ADF/destrin in complex with p210$^{bcr\text{-}abl}$ (Fig. 6*D*).

ADF/destrin is responsible for amoeboid motility

To further analyze the consequences of the isoform-specific recruitment of ADF for amoeboid motility, we modulated ADF/cofilin protein levels in Ba/F3p210 cells (Supplemental Fig. S3*A*, *B*). Myc-ADF/destrin-overexpressing Ba/F3p210 cells kept the same level of amoeboid motility (**Fig. 7*A***). In the same way, Myc-cofilin-1 overexpression did not affect the amoeboid motility of Ba/F3p210 cells (Fig. 7*A*). We subsequently explored the role of ADF and cofilin in p210$^{bcr\text{-}abl}$ induced amoeboid motility using siRNA (Supplemental Fig. S3*C*). Cofilin-1 silencing did not change the proportion of p210$^{bcr\text{-}abl}$ cells using amoeboid motility *vs.* control condition (Fig. 7*B* and Supplemental Movie S3). In contrast, ADF/destrin siRNA induced a complete loss of amoeboid motility type and a conversion to crawling and rolling type (Fig. 7*B* and Supplemental Movie S3). Using Ba/F3p210 cells embedded in 3D Matrigel, we studied the localization of cofilin-1 and ADF/destrin in addition to F-actin phalloidin labeling (Fig. 7*C*). We observed that cofilin-1 is relatively homogenously distributed in the cytoplasm, without polarization or clustering. In contrast, ADF/destrin concentrates in the leading edge and at a lower level in the tail of amoeboid cells. Interestingly, colocalization index of cofilin-1 with F-actin was lower (max: 0.60) than for ADF/destrin (max: 0.97), pointing out that ADF/destrin seems to interact more tightly with actin in this model. It has to be noted that disruption of the cortical actin in the cell body where contraction occurs, corresponds to ADF/destrin labeling. Notably, cells not embedded in Matrigel, which also display amoeboid phenotype, present a distribution of ADF/destrin and cofilin similar to that observed in 3D Matrigel (Fig. 7*D*). These results indicate a fundamental role for ADF/

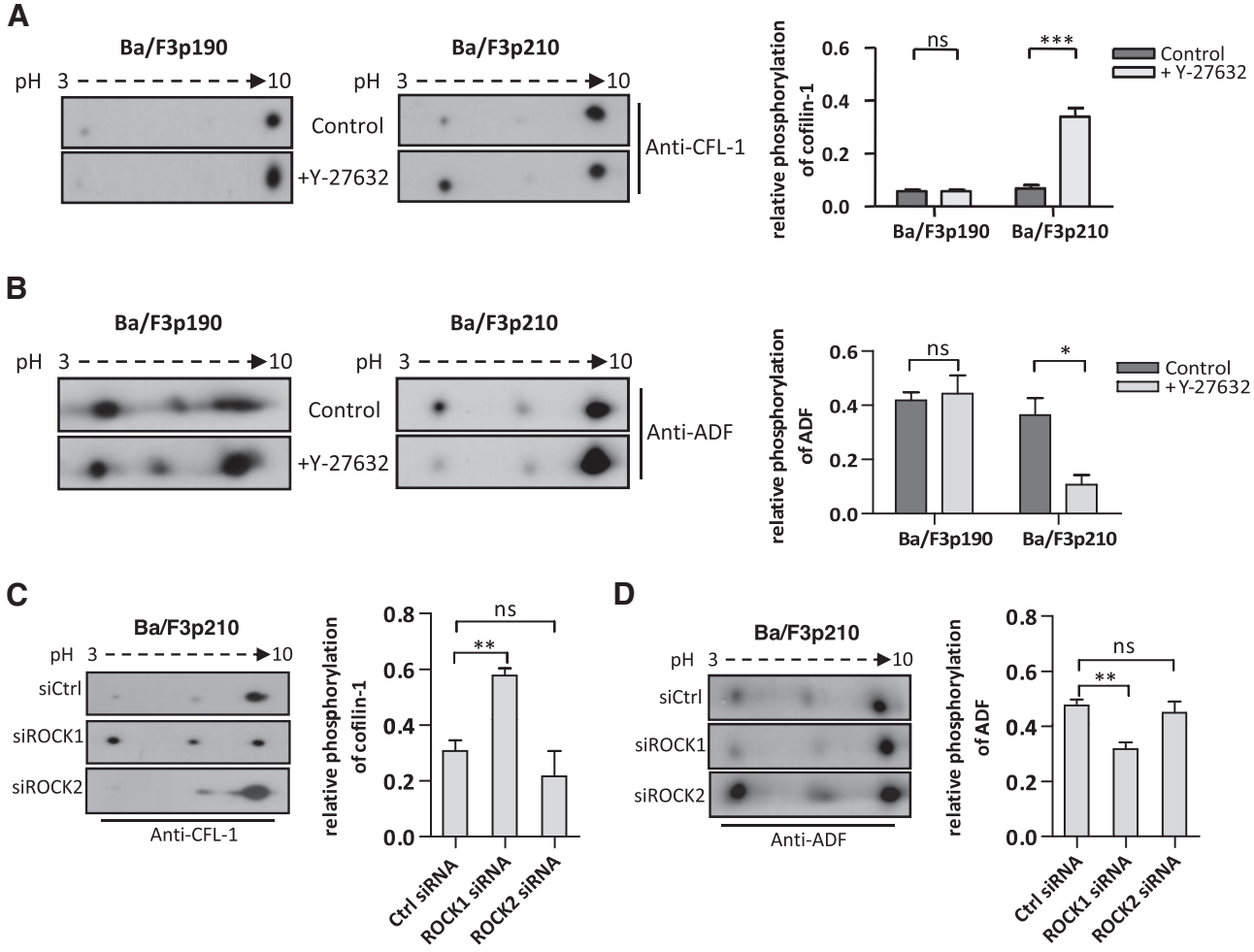

Figure 5. ROCK1 controls cofilin-1 and ADF/destrin phosphorylation only in Ba/F3p210 cells. *A*, *B*) Phosphorylation state of ADFs in p210$^{bcr\text{-}abl}$-expressing cells are dependent on ROCK1. 2D-PAGE followed by Western blot analysis of Ba/F3p190 and Ba/F3p210 cell extracts after 5 h of 10 μM Y-27632 treatment. Phosphorylated and unphosphorylated forms of cofilin-1 (*A*) and ADF/destrin (*B*) were detected by immunoblotting. *C*, *D*) 2D-PAGE followed by Western blot analysis of Ba/F3p210 cell extracts, 48 h after transfection with the indicated Rock isoform-specific siRNA. Phosphorylated and unphosphorylated forms of cofilin-1 (*C*) and ADF/destrin (*D*) were detected by immunoblotting. 2D results are expressed as mean ± SD values of 3 independent experiments (n=3). ns, nonsignificant. *$P < 0.05$, **$P < 0.01$, ***$P < 0.001$; unpaired Student's t test.

destrin in amoeboid motility. It has to be noted that the phospho-MyPT1 level is not modified by silencing cofilin-1 or ADF/destrin, suggesting the loss of amoeboid motility on ADF/destrin siRNA-treatment is not caused by altered myosin signaling (Fig. 7*E*). Together with data in Figs. 2 and 3, this indicates that the RhoA-ROCK-ADF pathway and the RhoA-ROCK-myosin pathway are both necessary but individually not sufficient to obtain amoeboid motility.

DISCUSSION

Amoeboid motility represents a major type of cell motility, largely used by hematopoietic cells and to some extent by tumor cells in dense matrices *in vivo* (21, 22). Despite its importance *in vivo*, the molecular mechanisms leading to amoeboid movements are still poorly understood, except it is generally accepted to be mediated by pathways downstream of Rho (21, 22). Using Bcr-Abl-expressing Ba/F3 cells, we unravel a new Rho-induced mechanism required for amoeboid motility. This consists in a specific regulation and function for the ADF/destrin in p210$^{bcr\text{-}abl}$ complex, distinct from its highly similar paralog cofilin-1 (31), complementary to the classical myosin II pathway.

We previously showed that Ba/F3p190 and or Ba/F3p210 display spontaneous motility but do so in different modes with the latter displaying amoeboid motility. We demonstrated that the DH/PH domain of p210$^{bcr\text{-}abl}$ specifically activates RhoA, and this activation is necessary for amoeboid motility (13). The central role of RhoA in amoeboid motility is generally accepted to act through actomyosin-based contraction (24, 35, 36). The exclusive ROCK-dependent MLC phosphorylation in Ba/F3p210 cells and nearly complete blockage of amoeboid motility on myosin inhibition (Fig. 3*D*) confirm this is also the case here. Intriguingly, we show this activation is exclusively dependent on ROCK1 signaling.

ROCK is a generally accepted key molecule in cell

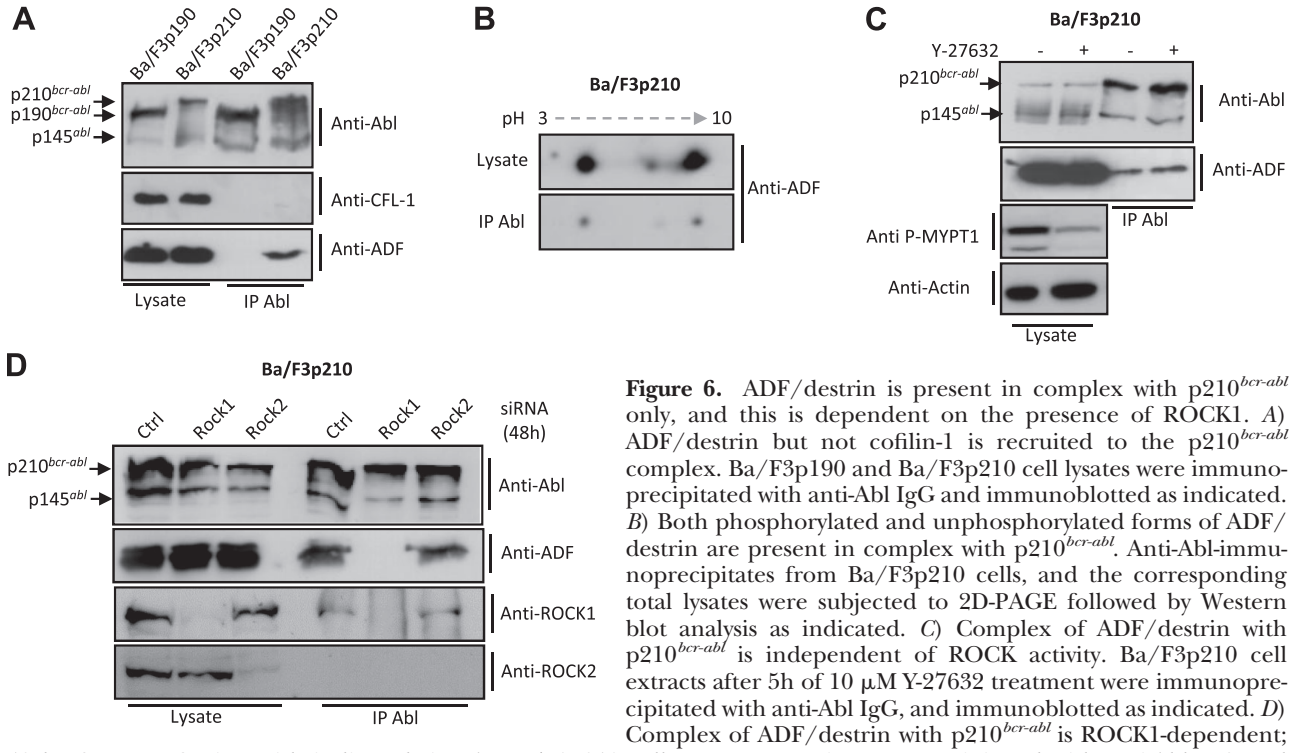

Figure 6. ADF/destrin is present in complex with p210$^{bcr\text{-}abl}$ only, and this is dependent on the presence of ROCK1. *A*) ADF/destrin but not cofilin-1 is recruited to the p210$^{bcr\text{-}abl}$ complex. Ba/F3p190 and Ba/F3p210 cell lysates were immunoprecipitated with anti-Abl IgG and immunoblotted as indicated. *B*) Both phosphorylated and unphosphorylated forms of ADF/destrin are present in complex with p210$^{bcr\text{-}abl}$. Anti-Abl-immunoprecipitates from Ba/F3p210 cells, and the corresponding total lysates were subjected to 2D-PAGE followed by Western blot analysis as indicated. *C*) Complex of ADF/destrin with p210$^{bcr\text{-}abl}$ is independent of ROCK activity. Ba/F3p210 cell extracts after 5h of 10 μM Y-27632 treatment were immunoprecipitated with anti-Abl IgG, and immunoblotted as indicated. *D*) Complex of ADF/destrin with p210$^{bcr\text{-}abl}$ is ROCK1-dependent; 48 h after transfection with indicated siRNA, Ba/F3p210 cell extracts were immunoprecipitated with anti-Abl IgG and immunoblotted as indicated.

migration, but a specific role for a ROCK isoform in a motility mode is not yet reported. ROCK1 (and not ROCK2) was shown to be a prime determinant in leukocyte recruitment after vascular injury in mice (37). Mouse genetics and isoform-specific down-regulation are starting to provide evidence for nonredundant functions and differential upstream and downstream partners (reviewed in ref. 38). Since ROCK1 and 2 are highly similar, and most commonly used ROCK inhibitors target both isoforms (39), insight into isoform-specific effects is only slowly emerging.

In Ba/F3p210 cells presenting constitutive Rho/ROCK1 activation, the presence of the actin binding protein ADF/destrin (and not cofilin 1) is also required for amoeboid motility, even on MLC activation. This makes ADF/destrin and myosin equally important to establish amoeboid movement. With myosin exerting contraction, and in line with the actin filament depolymerising activity of ADF/destrin, this suggests a specific and crucial role for ADF/destrin in actin disassembly and/or actin filament turnover in these cells. Although both signaling from Rho-ROCK to members of the ADF/cofilins (40, 41) and a role of ADF/cofilin members in motility are well documented (25, 31, 42), the determining role of ADF/destrin in amoeboid motility mode and the isoform-specificity hereof is novel. In general, Rho/ROCK signaling results in increased ADF/cofilin phosphorylation (40, 41) by activating cofilin kinases. In Ba/F3p210 cells, ROCK1 inhibition similarly results in a lower level of ADF/destrin phosphorylation. Importantly, the ADF/destrin phosphorylation level appears similar in Ba/F3p190 cells and ROCK inhibitor-treated Ba/F3p190 cells, indicating that ADF/destrin phosphorylation is under the control of different pathways in each cell type.

Within the ADF/cofilin family, isoform-specific function or regulation is even less understood. The 2 nonmuscle isoforms ADF (destrin) and cofilin-1 (n-cofilin) have been until now mostly considered functionally redundant (42). They indeed have very similar properties in relation to their main function, *i.e.*, modulating actin dynamics (43, 44), and this is likely the basis for reported compensatory role in cells (26) or mice (45, 46). They display tissue-specific expression levels during development and in adult organisms (43) with cofilin-1 most widely expressed and predominant in embryonic stages (43, 47). Cofilin-1 knockout is consequently embryonic lethal (47), whereas a destrin-null-mice has only mild phenotypes (32). Together this has led to the assumption that ADF/destrin is a minor isoform, and the role of its coexpression with cofilin-1 in multiple cell types remains largely unknown and little studied. To our knowledge, only 1 report previously described a nonredundant function for mammalian ADF/destrin and cofilin-1 in migration (32).

We identified ROCK1 and ADF/destrin as two new and specific components of the p210$^{bcr\text{-}abl}$ "signalplex" and the existence of RhoA-ROCK1-ADF/destrin signaling with high isoform specifity. Indeed, these two proteins are not associated with p190$^{bcr\text{-}abl}$, nor was cofilin-1 or ROCK2 present in the p210$^{bcr\text{-}abl}$ complex. The recruitment of these partners is probably linked to the Rho-GEF activity of p210$^{bcr\text{-}abl}$ since ROCK1 is not present in complex with the p210S509A mutant of p210$^{bcr\text{-}abl}$ (Supplemental Fig. S1*A* and ref. 13). Bcr-Abl has been extensively described as a scaffolding protein, the number and qualities of partners increasing regu-

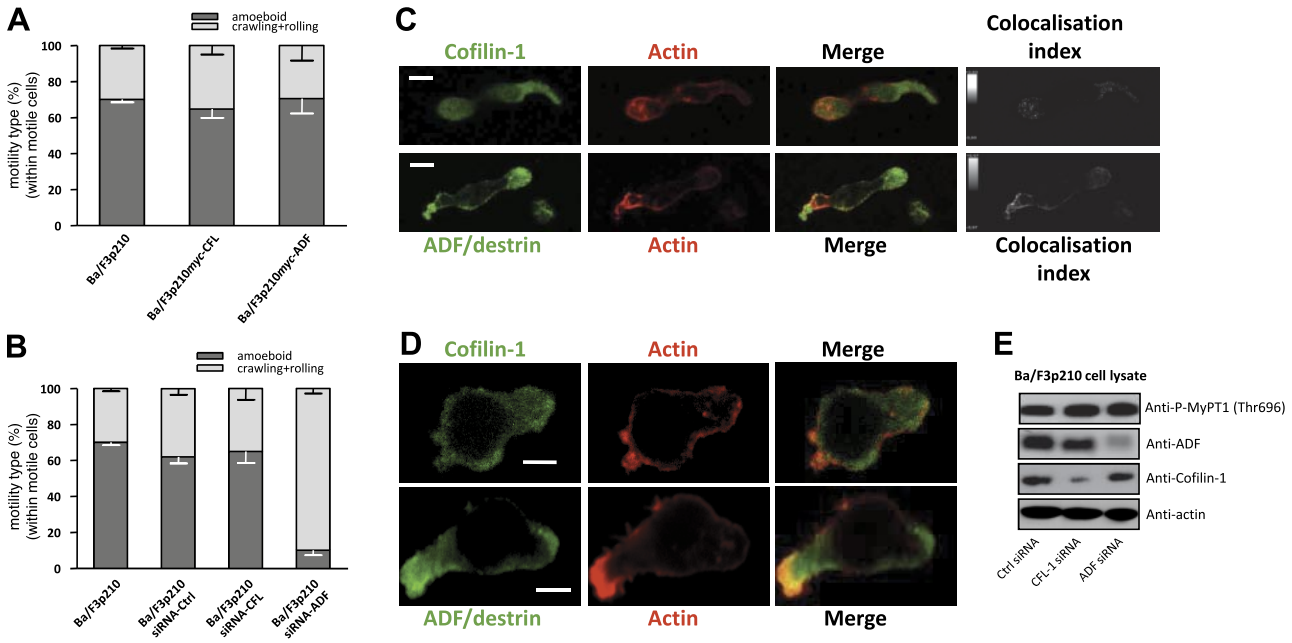

Figure 7. ADF/destrin is strongly required for amoeboid motility in p210$^{bcr\text{-}abl}$-expressing cells. *A*) Overexpression of *myc*-tagged ADF or *myc*-tagged cofilin-1 does not modify the motility type of motile p210$^{bcr\text{-}abl}$ cells. Analysis of time-lapse recordings in 3D Matrigel of Ba/F3p210 stably transfected with either *myc*-ADF or *myc*-cofilin-1. Motile cells were sorted in amoeboid or crawling/rolling motility type and expressed as percentage of motile Ba/F3p210 cells; 200-600 cells/condition were observed. *B*) ADF/destrin but not cofilin-1 down-regulation abrogates the amoeboid motility of p210$^{bcr\text{-}abl}$-expressing cells. Analysis of time-lapse recordings of control, ADF, or cofilin-1 siRNA-transfected Ba/F3p210 cell; 48 h after transfection with the indicated siRNA, Ba/F3p210 cells were embedded into 3D Matrigel, and time-lapse recordings were performed using DIC microscopy. *C*) Localization of ADFs in Matrigel-embedded Ba/F3p210 cells. Ba/F3p210 cells were embedded in Matrigel for 12 h, then fixed, stained for F-actin with phalloidin-alexa-546 and for cofilin-1 or ADF/destrin with specific antibody coupled with secondary antibody-alexa-488. Representative confocal images obtained with epifluorescence for cofilin-1 or ADF/destrin (green), actin (red), or a combination of the two (merge) are shown. *D*) Localization of ADFs in adhesion-free Ba/F3p210 cells. Ba/F3p210 cells in suspension were fixed, stained for F-actin with phalloidin-alexa-546 and for cofilin-1 or ADF/destrin with specific antibody coupled with secondary antibody-alexa-488. Representative confocal images obtained with epifluorescence for cofilin-1 or ADF/destrin (green), actin (red), or a combination of the 2 (merge) are shown *E*) Myosin II pathway is still activated in siRNA-ADF expressing cells. P-MYPT level on ADF and CFL-1 siRNA knockdowns probed by immunoblotting total proteins from indicated extracts. ADF and cofilin-1 siRNA-knockdowns show no cross-reactivity 48 h post-transfection. Scale bars = 5 μm.

larly (48). Intriguingly, the presence of ADF/destrin in the p210$^{bcr\text{-}abl}$ complex requires ROCK1, but not its activity (Fig. 6*C*). Indeed, only knockdown of ROCK1 prevented the anchorage of ADF/destrin to the complex (Fig. 6*D*). In addition, the presence of both ADF/destrin and phosphorylated ADF/destrin in the complex suggests that its association to the p210$^{bcr\text{-}abl}$ complex is independent of ADF/destrin phosphorylation status, further suggesting its activity may cycle within the complex. It remains to be shown whether the recruitment of ADF/destrin to the p210$^{bcr\text{-}abl}$ complex is controlling local *vs.* global ADF/destrin activity ratios, as, *e.g.*, shown in ref. 49.

Our main observation is that p210$^{bcr\text{-}abl}$ cells lose amoeboid motility only when the level of ADF/destrin, and not that of cofilin 1, is down-regulated. Together with the exclusive recruitment of ADF/destrin to the p210$^{bcr\text{-}abl}$ complex and the observation of a similar phosphorylation level of ADF/destrin in p210$^{bcr\text{-}abl}$ *vs.* p190$^{bcr\text{-}abl}$ cells, this suggests the p210$^{bcr\text{-}abl}$ complex (implying spatially enriched Rho-ROCK1 signaling) may be able inducing a (local) response on actin dynamics that is crucial for establishing the amoeboid motility mode. Amoeboid movement is characterized by a protruding cell front, accompanied with contractions of the cell body, and, in contrast to the mesenchymal mode of migration, myosin-mediated contraction of the cell rear and actin flowing at the leading edge are spatiotemporally uncoupled (19, 50). This uncoupling may explain why both myosin and ADF/destrin activity are required for amoeboid motility. Ba/F3p210 cells, like normal hematopoietic motile cells, extrude a large and dynamic pseudopod, which plays the role of a leading edge for the cell body to move in the same direction. Amoeboid translocation is then the result of contraction of the cell body toward the membrane protrusion *via* actomyosin activity and actin remodelling (19), and we suggest that ADF/destrin participates in this. Interestingly, we found ADF/destrin clustered in these protrusions, and it is also more cortical in the cell body than cofilin-1, suggesting that ADF/destrin concentrates in the sites of actin flowing and of acto-myosin contraction. Of note, this appears different from amoeboid motility based on membrane blebbing (21, 51), characteristic of *Dictyostelium discoideum* (20) or some solid tumor cells undergoing amoeboid transition (36, 52, 53).

Despite the determining role of ADF/destrin, the function of cofilin-1 in the amoeboid moving p210$^{bcr\text{-}abl}$ cells

should also be explored. Cofilin-1 has already been shown to play an important role during leukocyte chemotaxis (54–56). The global activity level of cofilin-1 is similar in p190 and p210 cells, and cofilin-1 is not recruited to either Bcr-Abl complex. Surprisingly, cofilin-1 phosphorylation is increased on ROCK1 inhibition in p210 cells, emphasizing ADF/cofilin isoform specificity. Further work on ADF/destrin and cofilin-1 localization studies may provide answers on how these isoforms differ in spatial and temporal regulation of actin reorganization.

Evidence has been raised that amoeboid transition of mesenchymal cells is the consequence of a shift from a Rac-induced (mesenchymal) motility to a RhoA-induced mode of motility (23, 52, 57). The originality of the $p210^{bcr\text{-}abl}$ model lies in the fact that we observe Rho activation on top of Rac activity, and both are necessary to obtain migration through amoeboid motility (13). It will be of interest to further determine to what extent these pathways interact and employ isoform-specific activities in function of changing motility modes.

Bcr-Abl-expressing cells have been shown to be independent from chemotaxis, particularly SDF-1α-induced ones (11). Together with the loss of chemokine regulation, the spontaneous motility of Bcr-Abl-expressing cells may favor the escape from stromal regulation. This may contribute to the oncogenicity of Bcr-Abl through a prominent role of Rho-GTPases. Recent literature has focused on Rac in CML leukemogenesis (58). Also, the hyperactivation of Cdc42 by $p210^{bcr\text{-}abl}$ has been involved in the loss of directionality of these cells (9). Our data finally demonstrate that RhoA triggers spontaneous amoeboid motility in Bcr-Abl-transformed cells. Altogether, these elements indicate a major role for Rho-GTPases in Bcr-Abl-induced leukemias, positioning them as interesting targets for alternative treatments.

In summary, a main contribution of this work is the identification of ADF/destrin, together with ROCK1, as specific components of the $p210^{bcr\text{-}abl}$ complex, and as determinants that drive amoeboid motility in an hematopoietic cell model. This effect is isoform specific, and ADF/destrin acts in conjunction with RhoA-ROCK1-MLC-myosin activity to induce amoeboid motility. This study also underscores the need for a closer study of the specific activities of cofilin/ADF members in other cellular functions and systems. Moreover, the effect of spontaneous migration through amoeboid motility may be important in chronic myelogenous leukemia pathogenesis, particularly in the context of an altered crosstalk of hematopoietic cells with the microenvironment. FJ

The authors thank Nathalie Piccirilli for efficient technical help with cell cultures and Anne Cantereau for the microscopy platform ImageUP. This work was realized using grants from the Ligue Nationale Contre le Cancer (Vienne, Charente-Maritime, Deux-Sèvres, Loir-et-Cher), Sport et Collection, and Association Pictave pour l'Etude des Maladies du SAng (APEMSA). The authors declare no conflicts of interest.

REFERENCES

1. Ren, R. (2005) Mechanisms of BCR-ABL in the pathogenesis of chronic myelogenous leukaemia. *Nat. Rev. Cancer* **5,** 172–183
2. Daley, G. Q., Van Etten, R. A., and Baltimore, D. (1990) Induction of chronic myelogenous leukemia in mice by the P210bcr/abl gene of the Philadelphia chromosome. *Science* **247,** 824–830
3. Clark, S. S., McLaughlin, J., Timmons, M., Pendergast, A. M., Ben-Neriah, Y., Dow, L. W., Crist, W., Rovera, G., Smith, S. D., and Witte, O. N. (1988) Expression of a distinctive BCR-ABL oncogene in Ph1-positive acute lymphocytic leukemia (ALL). *Science* **239,** 775–777
4. Ilaria, R. L., Jr., and Van Etten, R. A. (1996) p210 and p190(BCR/ABL) induce the tyrosine phosphorylation and DNA binding activity of multiple specific STAT family members. *J. Biol. Chem.* **271,** 31704–31710
5. Lugo, T. G., Pendergast, A. M., Muller, A. J., and Witte, O. N. (1990) Tyrosine kinase activity and transformation potency of bcr-abl oncogene products. *Science* **247,** 1079–1082
6. Salgia, R., Li, J. L., Ewaniuk, D. S., Pear, W., Pisick, E., Burky, S. A., Ernst, T., Sattler, M., Chen, L. B., and Griffin, J. D. (1997) BCR/ABL induces multiple abnormalities of cytoskeletal function. *J. Clin. Invest.* **100,** 46–57
7. Wertheim, J. A., Perera, S. A., Hammer, D. A., Ren, R., Boettiger, D., and Pear, W. S. (2003) Localization of BCR-ABL to F-actin regulates cell adhesion but does not attenuate CML development. *Blood* **102,** 2220–2228
8. Fierro, F. A., Taubenberger, A., Puech, P. H., Ehninger, G., Bornhauser, M., Muller, D. J., and Illmer, T. (2008) BCR/ABL expression of myeloid progenitors increases beta1-integrin mediated adhesion to stromal cells. *J. Mol. Biol.* **377,** 1082–1093
9. Chang, Y. C., Tien, S. C., Tien, H. F., Zhang, H., Bokoch, G. M., and Chang, Z. F. (2009) p210(Bcr-Abl) desensitizes Cdc42 GTPase signaling for SDF-1alpha-directed migration in chronic myeloid leukemia cells. *Oncogene* **28,** 4105–4115
10. Geay, J. F., Buet, D., Zhang, Y., Foudi, A., Jarrier, P., Berthebaud, M., Turhan, A. G., Vainchenker, W., and Louache, F. (2005) p210BCR-ABL inhibits SDF-1 chemotactic response via alteration of CXCR4 signaling and down-regulation of CXCR4 expression. *Cancer Res.* **65,** 2676–2683
11. Salgia, R., Quackenbush, E., Lin, J., Souchkova, N., Sattler, M., Ewaniuk, D. S., Klucher, K. M., Daley, G. Q., Kraeft, S. K., Sackstein, R., Alyea, E. P., von Andrian, U. H., Chen, L. B., Gutierrez-Ramos, J. C., Pendergast, A. M., and Griffin, J. D. (1999) The BCR/ABL oncogene alters the chemotactic response to stromal-derived factor-1alpha. *Blood* **94,** 4233–4246
12. Peled, A., Hardan, I., Trakhtenbrot, L., Gur, E., Magid, M., Darash-Yahana, M., Cohen, N., Grabovsky, V., Franitza, S., Kollet, O., Lider, O., Alon, R., Rechavi, G., and Lapidot, T. (2002) Immature leukemic CD34+CXCR4+ cells from CML patients have lower integrin-dependent migration and adhesion in response to the chemokine SDF-1. *Stem Cells* **20,** 259–266
13. Daubon, T., Chasseriau, J., El Ali, A., Rivet, J., Kitzis, A., Constantin, B., and Bourmeyster, N. (2008) Differential motility of p190bcr-abl- and p210bcr-abl-expressing cells: respective roles of Vav and Bcr-Abl GEFs. *Oncogene* **27,** 2673–2685
14. Harnois, T., Constantin, B., Rioux, A., Grenioux, E., Kitzis, A., and Bourmeyster, N. (2003) Differential interaction and activation of Rho family GTPases by p210bcr-abl and p190bcr-abl. *Oncogene* **22,** 6445–6454
15. Raftopoulou, M., and Hall, A. (2004) Cell migration: Rho GTPases lead the way. *Dev. Biol.* **265,** 23–32
16. Jaffe, A. B., and Hall, A. (2005) Rho GTPases: biochemistry and biology. *Annu. Rev. Cell Dev. Biol.* **21,** 247–269
17. Ladwein, M., and Rottner, K. (2008) On the Rho'd: the regulation of membrane protrusions by Rho-GTPases. *FEBS Lett.* **582,** 2066–2074
18. Pellegrin, S., and Mellor, H. (2007) Actin stress fibres. *J. Cell Sci.* **120,** 3491–3499
19. Lammermann, T., and Sixt, M. (2009) Mechanical modes of 'amoeboid' cell migration. *Curr. Opin. Cell Biol.* **21,** 636–644
20. Yoshida, K., and Soldati, T. (2006) Dissection of amoeboid movement into two mechanically distinct modes. *J. Cell Sci.* **119,** 3833–3844
21. Mandeville, J. T., Lawson, M. A., and Maxfield, F. R. (1997) Dynamic imaging of neutrophil migration in three dimensions: mechanical interactions between cells and matrix. *J. Leukoc. Biol.* **61,** 188–200

22. Friedl, P., and Wolf, K. (2003) Tumour-cell invasion and migration: diversity and escape mechanisms. *Nat. Rev. Cancer* **3,** 362–374
23. Sahai, E., and Marshall, C. J. (2003) Differing modes of tumour cell invasion have distinct requirements for Rho/ROCK signalling and extracellular proteolysis. *Nat. Cell Biol.* **5,** 711–719
24. Gadea, G., de Toledo, M., Anguille, C., and Roux, P. (2007) Loss of p53 promotes RhoA-ROCK-dependent cell migration and invasion in 3D matrices. *J. Cell Biol.* **178,** 23–30
25. Wyckoff, J. B., Pinner, S. E., Gschmeissner, S., Condeelis, J. S., and Sahai, E. (2006) ROCK- and myosin-dependent matrix deformation enables protease-independent tumor-cell invasion in vivo. *Curr. Biol.* **16,** 1515–1523
26. Hotulainen, P., Paunola, E., Vartiainen, M. K., and Lappalainen, P. (2005) Actin-depolymerizing factor and cofilin-1 play overlapping roles in promoting rapid F-actin depolymerization in mammalian nonmuscle cells. *Mol. Biol. Cell* **16,** 649–664
27. Sixt, M., and Lammermann, T. (2010) In vitro analysis of chemotactic leukocyte migration in 3D environments. *Methods Mol. Biol.* **769,** 149–165
28. Unwin, R. D., Sternberg, D. W., Lu, Y., Pierce, A., Gilliland, D. G., and Whetton, A. D. (2005) Global effects of BCR/ABL and TEL/PDGFRbeta expression on the proteome and phosphoproteome: identification of the Rho pathway as a target of BCR/ABL. *J. Biol. Chem.* **280,** 6316–6326
29. Lee, C. F., Griffiths, S., Rodriguez-Suarez, E., Pierce, A., Unwin, R. D., Jaworska, E., Evans, C. A. J., Gaskell, S., and Whetton, A. D. (2010) Assessment of downstream effectors of BCR/ABL protein tyrosine kinase using combined proteomic approaches. *Proteomics* **10,** 3321–3342
30. Kimura, K., Ito, M., Amano, M., Chihara, K., Fukata, Y., Nakafuku, M., Yamamori, B., Feng, J., Nakano, T., Okawa, K., Iwamatsu, A., and Kaibuchi, K. (1996) Regulation of myosin phosphatase by Rho and Rho-associated kinase (Rho-kinase). *Science* **273,** 245–248
31. Van Troys, M., Huyck, L., Leyman, S., Dhaese, S., Vandekerkhove, J., and Ampe, C. (2008) Ins and outs of ADF/cofilin activity and regulation. *Eur. J. Cell Biol.* **87,** 649–667
32. Estornes, Y., Gay, F., Gevrey, J. C., Navoizat, S., Nejjari, M., Scoazec, J. Y., Chayvialle, J. A., Saurin, J. C., and Abello, J. (2007) Differential involvement of destrin and cofilin-1 in the control of invasive properties of Isreco1 human colon cancer cells. *Int. J. Cancer* **121,** 2162–2171
33. Kuzelova, K., and Hrkal, Z. (2008) Rho-signaling pathways in chronic myelogenous leukemia. *Cardiovasc. Hematol. Disord. Drug Targets* **8,** 261–267
34. Ghosh, M., Song, X., Mouneimne, G., Sidani, M., Lawrence, D. S., and Condeelis, J. S. (2004) cofilin promotes actin polymerization and defines the direction of cell motility. *Science* **304,** 743–746
35. Friedl, P. (2004) Prespecification and plasticity: shifting mechanisms of cell migration. *Curr. Opin. Cell Biol.* **16,** 14–23
36. Pinner, S., and Sahai, E. (2008) PDK1 regulates cancer cell motility by antagonising inhibition of ROCK1 by RhoE. *Nat. Cell Biol.* **10,** 127–137
37. Noma, K., Rikitake, Y., Oyama, N., Yan, G., Alcaide, P., Liu, P. Y., Wang, H., Ahl, D., Sawada, N., Okamoto, R., Hiroi, Y., Shimizu, K., Luscinskas, F. W., Sun, J., and Liao, J. K. (2008) ROCK1 mediates leukocyte recruitment and neointima formation following vascular injury. *J. Clin. Invest.* **118,** 1632–1644
38. Shi, J., Zhang, L., and Wei, L. (2011) Rho-kinase in development and heart failure: insights from genetic models. *Pediatr. Cardiol.* **32,** 297–304
39. Amano, M., Nakayama, M., and Kaibuchi, K. (2010) Rho-kinase/ROCK: a key regulator of the cytoskeleton and cell polarity. *Cytoskeleton (Hoboken)* **67,** 545–554
40. Amano, T., Tanabe, K., Eto, T., Narumiya, S., and Mizuno, K. (2001) LIM-kinase 2 induces formation of stress fibres, focal adhesions and membrane blebs, dependent on its activation by Rho-associated kinase-catalysed phosphorylation at threonine-505. *Biochem. J.* **354,** 149–159
41. Bernard, O. (2007) Lim kinases, regulators of actin dynamics. *Int. J. Biochem. Cell Biol.* **39,** 1071–1076
42. Bernstein, B. W., and Bamburg, J. R. (2010) ADF/cofilin: a functional node in cell biology. *Trends Cell Biol.* **20,** 187–195
43. Vartiainen, M. K., Mustonen, T., Mattila, P. K., Ojala, P. J., Thesleff, I., Partanen, J., and Lappalainen, P. (2002) The three mouse actin-depolymerizing factor/cofilins evolved to fulfill cell-type-specific requirements for actin dynamics. *Mol. Biol. Cell* **13,** 183–194
44. Yeoh, S., Pope, B., Mannherz, H. G., and Weeds, A. (2002) Determining the differences in actin binding by human ADF and cofilin. *J. Mol. Biol.* **315,** 911–925
45. Kuure, S., Cebrian, C., Machingo, Q., Lu, B.C., Chi, X., Hyink, D., D'Agati, V., Gurniak, C., Witke, W., and Costantini, F. (2010) Actin depolymerizing factors cofilin1 and destrin are required for ureteric bud branching morphogenesis. *PLoS Genet.* **6,** e1001176
46. Gorlich, A., Wolf, M., Zimmermann, A. M., Gurniak, C. B., Al Banchaabouchi, M., Sassoe-Pognetto, M., Witke, W., Friauf, E., and Rust, M. B. (2011) N-cofilin can compensate for the loss of ADF in excitatory synapses. *PLoS ONE* **6,** e26789
47. Gurniak, C. B., Perlas, E., and Witke, W. (2005) The actin depolymerizing factor n-cofilin is essential for neural tube morphogenesis and neural crest cell migration. *Dev. Biol.* **278,** 231–241
48. Quintas-Cardama, A., and Cortes, J. (2009) Molecular biology of bcr-abl1-positive chronic myeloid leukemia. *Blood* **113,** 1619–1630
49. Wen, Z., Han, L., Bamburg, J. R., Shim, S., Ming, G. L., and Zheng, J. Q. (2007) BMP gradients steer nerve growth cones by a balancing act of LIM kinase and Slingshot phosphatase on ADF/cofilin. *J. Cell Biol.* **178,** 107–119
50. Lämmermann, T., Bader, B. L., Monkley, S. J., Worbs, T., Wedlich-Soldner, R., Hirsch, K., Förster, R., Critchley, D. R., Fässler, R., and Sixt, M. (2008) Rapid leukocyte migration by integrin-independent flowing and squeezing. *Nature* **453,** 51–55
51. Wolf, K., Muller, R., Borgmann, S., Brocker, E. B., and Friedl, P. (2003) Amoeboid shape change and contact guidance: T-lymphocyte crawling through fibrillar collagen is independent of matrix remodeling by MMPs and other proteases. *Blood* **102,** 3262–3269
52. Torka, R., Thuma, F., Herzog, V., and Kirfel, G. (2006) ROCK signaling mediates the adoption of different modes of migration and invasion in human mammary epithelial tumor cells. *Exp. Cell Res.* **312,** 3857–3871
53. Wilkinson, S., Paterson, H. F., and Marshall, C. J. (2005) Cdc42-MRCK and Rho-ROCK signalling cooperate in myosin phosphorylation and cell invasion. *Nat. Cell Biol.* **7,** 255–261
54. Okada, K., Takano-Ohmuro, H., Obinata, T., and Abe, H. (1996) Dephosphorylation of cofilin in polymorphonuclear leukocytes derived from peripheral blood. *Exp. Cell Res.* **227,** 116–122
55. Hirayama, A., Adachi, R., Otani, S., Kasahara, T., and Suzuki, K. (2007) cofilin plays a critical role in IL-8-dependent chemotaxis of neutrophilic HL-60 cells through changes in phosphorylation. *J. Leukoc. Biol.* **81,** 720–728
56. Klemke, M., Kramer, E., Konstandin, M. H., Wabnitz, G. H., and Samstag, Y. (2010) An MEK-cofilin signalling module controls migration of human T cells in 3D but not 2D environments. *EMBO J.* **29,** 2915–2929
57. Sanz-Moreno, V., Gadea, G., Ahn, J., Paterson, H., Marra, P., Pinner, S., Sahai, E., and Marshall, C. J. (2008) Rac activation and inactivation control plasticity of tumor cell movement. *Cell* **135,** 510–523
58. Thomas, E. K., Cancelas, J. A., Chae, H. D., Cox, A. D., Keller, P. J., Perrotti, D., Neviani, P., Druker, B. J., Setchell, K. D., Zheng, Y., Harris, C. E., and Williams, D. A. (2007) Rac guanosine triphosphatases represent integrating molecular therapeutic targets for BCR-ABL-induced myeloproliferative disease. *Cancer Cell* **12,** 467–478

Received for publication February 22, 2012.
Accepted for publication September 17, 2012.